Nitric Oxide Inhibition of Lipid Peroxidation: Kinetics of Reaction with Lipid Peroxyl Radicals and Comparison with α-Tocopherol†

Valerie B. O'Donnell,‡ Phillip H. Chumley,‡ Neil Hogg,§ Allison Bloodsworth,‡ Victor M. Darley-Usmar,|| and Bruce A. Freeman*,‡

Departments of Anesthesiology, Biochemistry, Molecular Genetics, and Pathology and the UAB Center for Free Radical Biology, University of Alabama at Birmingham, Birmingham, Alabama 35233, and Biophysics Research Institute, Medical College of Wisconsin, 8701 Watertown Plank Road, Milwaukee, Wisconsin 53226

Received August 1, 1997; Revised Manuscript Received October 2, 1997⊗

ABSTRACT: The reaction between nitric oxide (•NO) and lipid peroxyl radicals (LOO•) has been proposed to account for the potent inhibitory properties of •NO toward lipid peroxidation processes; however, the mechanisms of this reaction, including kinetic parameters and nature of termination products, have not been defined. Here, the reaction between linoleate peroxyl radicals and •NO was examined using 2,2′-azobis(2-amidinopropane) hydrochloride-dependent oxidation of linoleate. Addition of •NO (0.5−20 μM) to peroxidizing lipid led to cessation of oxygen uptake, which resumed at original rates when all •NO had been consumed. At high •NO concentrations (>3 μM), the time of inhibition (T_{inh}) of chain propagation became increasingly dependent on oxygen concentration, due to the competing reaction of oxygen with •NO. Kinetic analysis revealed that a simple radical−radical termination reaction (•NO:ROO• = 1:1) does not account for the inhibition of lipid oxidation by •NO, and at least two molecules of •NO are consumed per termination reaction. A mechanism is proposed whereby •NO first reacts with LOO• ($k = 2 \times 10^9$ M^{-1} s^{-1}) to form LOONO. Following decomposition of LOONO to LO• and •NO_2, a second •NO is consumed via reaction with LO•, with the composite rate constant for this reaction being $k = 7 \times 10^4$ M^{-1} s^{-1}. At equal concentrations, greater inhibition of oxidation was observed with •NO than with α-tocopherol. Since •NO reacts with LOO• at an almost diffusion-limited rate, steady state concentrations of 30 nM •NO would effectively compete with endogenous α-tocopherol concentrations (about 20 μM) as a scavenger of LOO• in the lipid phase. This indicates that biological •NO concentrations (up to 2 μM) will significantly influence peroxidation reactions in vivo.

Nitric oxide (•NO)[1] is an endothelial-derived relaxation factor that modulates blood pressure and mediates a variety of biological actions, ranging from platelet activation and aggregation to neurotransmission and pathogen killing. The biological chemistry of this free radical is dominated by radical−radical reactions. For example, reactions of •NO with other free radical species lead to either inhibition or potentiation of oxidative damage. Inhibition of •NO synthase can substantially protect against tissue injury observed in both acute and chronic inflammation (*1*−*3*). Conversely, damage observed during myocardial reoxygenation injury has been directly attributed to •NO (*4*). Interestingly, cogeneration of •NO and O_2•$^-$ results in lipid oxidation via formation of the potent oxidant peroxynitrite ($ONOO^-$) (*5*). The reaction of •NO with peroxidizing lipid mixtures, in the absence of O_2•$^-$, leads to inhibition of oxidation (*6*−*10*). In contrast, when lipid peroxidation is initiated by O_2•$^-$ (i.e. metal-dependent decomposition of H_2O_2), a bell-shaped dose−response curve is observed for •NO (*8*). At low •NO:O_2•$^-$ (<1), increasing rates of •NO production enhance peroxidation, via increased rates of $ONOO^-$ formation. Once •NO:O_2•$^-$ equals or exceeds unity, •NO inhibits oxidation, by reacting with and removing $ONOO^-$ and presumably by terminating lipid radical-mediated chain propagation reactions (*11*).

The mechanism by which •NO inhibits lipid peroxidation has been postulated to involve reaction between •NO and lipid-derived radicals [e.g. lipid peroxyl (LOO•) or alkoxyl (LO•)] (*8*, *9*), on the basis of evidence obtained using peroxyl radicals with chemical characteristics very different from LOO•. However, the kinetics of the reaction between •NO and LOO• leading to chain termination has not been directly studied. In biological systems, •NO-dependent inhibition of peroxidation could be due to a number of reactions in addition to radical−radical chain termination. Nitric oxide can bind to metal centers to form redox inactive nitrosyl complexes (*12*) and, in high concentrations, can inactivate

† This work was supported by NIH Grants PO1 HL40456 and RO1 HL51245 (B.A.F., V.D.U.) and the Parker B. Francis Foundation (V.B.O.).

* Address correspondence to this author at 946 Tinsley Harrison Tower, 1900 Nineteenth St. S. University of Alabama at Birmingham, Birmingham, AL 35233 [telephone (205) 934-4234; fax (205) 934-7437; e-mail Bruce.Freeman@ccc.uab.edu].

‡ Departments of Anesthesiology, Biochemistry, and Molecular Genetics.

§ Biophysics Research Institute.

|| Department of Pathology.

⊗ Abstract published in *Advance ACS Abstracts,* November 15, 1997.

[1] Abbreviations: ABAP, 2′,2′-azobis(2-amidinopropane)hydrochloride; AMVN, 2,2′-azobis(2,4-dimethylvaleronitrile); DTPA, diethylenetriaminepentaacetic acid; BHT, butylated hydroxytoluene; •NO, nitric oxide; ABAP, A−N═N−A; A•, ABAP alkyl radical; AOO•, ABAP peroxyl radical; LH, unsaturated lipid; AOOH, ABAP hydroperoxide; L•, lipid alkyl radical; LOO•, lipid peroxyl radical; LOOH, lipid hydroperoxide; •NO_2, nitrogen dioxide; ArOH, antioxidant; use of the prefix "R" (e.g. in ROOH or $RONO_2$) denotes a functional group that may derive from either linoleate or ABAP; however, "L" refers to lipid and "A" refers to ABAP-derived chemical species.

S0006-2960(97)01891-6 CCC: $14.00

Table 1: Rate Constants Used for Kinetic Simulation of ABAP Oxidation of Linoleate

reaction	rate constant	ref
initiation		
(1) A—N═N—A → $2A^{\bullet} + N_2$	1.3×10^{-6} s^{-1}	33
(2) $A^{\bullet} + O_2 \rightarrow AOO^{\bullet}$	2×10^{9} M^{-1} s^{-1}	33
propagation		
(3) $AOO^{\bullet} + LH \rightarrow AOOH + L^{\bullet}$	1.27×10^{3} M^{-1} s^{-1}	calcd herein
(4) $L^{\bullet} + O_2 \rightarrow LOO^{\bullet}$	3×10^{8} M^{-1} s^{-1}	34
(5) $LOO^{\bullet} + LH \rightarrow LOOH + L^{\bullet}$	1.27×10^{3} M^{-1} s^{-1}	calcd herein
termination		
(6) $L^{\bullet} + L^{\bullet} \rightarrow$ L—L	5×10^{8} M^{-1} s^{-1}	34
(7) $L^{\bullet} + LOO^{\bullet} \rightarrow$ LOOL	5×10^{7} M^{-1} s^{-1}	34
(8) $LOO^{\bullet} + LOO^{\bullet} \rightarrow LOOL + O_2$	10^{7} M^{-1} s^{-1}	34
nitric oxide		
(9) $^{\bullet}NO + LOO^{\bullet} \rightarrow$ ROONO	2×10^{9} M^{-1} s^{-1}	14
(10) $^{\bullet}NO + AOO^{\bullet} \rightarrow$ ROONO	2×10^{9} M^{-1} s^{-1}	14
(11) $4^{\bullet}NO + O_2 + 2H_2O \rightarrow 4NO_2^- + 4H^+$	6×10^{6} M^{-2} s^{-1}	32
(12) $^{\bullet}NO +$ ROONO → RONO	ranged from 0 to 2×10^{9} M^{-1} s^{-1}	25

initiators of lipid peroxidation, such as lipoxygenase (*13*).

The kinetics and mechanism of reaction between $^{\bullet}NO$ and $LOO^{\bullet}$ were examined using the azo initiator compounds 2′2′-azobis(2-amidinopropane) hydrochloride (ABAP) and 2,2′-azobis(2,4-dimethylvaleronitrile) (AMVN). Azo initiators were chosen to (a) allow lipid peroxidation to occur in the complete absence of transition metal ions by use of a chelator, thus ensuring that $LO^{\bullet}$ is not generated, (b) provide a linear rate of initiation, leading to controlled quantitative formation of LOOH from LH and O_2, (c) limit $^{\bullet}NO$ reaction with O_2 and avoid $^{\bullet}NO$ reaction with $O_2^{\bullet-}$, thus ensuring that the production of other potential oxidizing/nitrating species ($ONOO^-$, NO_2, N_2O_3) is minimized, and (d) take advantage of the well-established kinetic behavior of these reactions.

Here, we report that the inhibition of lipid peroxidation by $^{\bullet}NO$ occurs with a rate constant consistent with that determined for the reaction between $^{\bullet}NO$ and other alkyl peroxyl radicals [i.e. $(1-3) \times 10^{9}$ M^{-1} s^{-1} (*14*)]; however, the inhibitory mechanism is more complex than the simple radical−radical termination reaction between $^{\bullet}NO$ and $LOO^{\bullet}$ as two to three molecules of $^{\bullet}NO$ are consumed per termination reaction. The chain termination reaction of $^{\bullet}NO$ toward peroxyl radicals proceeds with a faster rate constant than that mediated by α-tocopherol, the major biological lipophilic antioxidant, and is expected to occur in vivo.

EXPERIMENTAL PROCEDURES

Materials. All chemicals were from Sigma Chemical Co. (St. Louis, MO), unless otherwise stated. Lipids were from Nu-Chek Prep (Elysian, MI). ABAP and AMVN were from Wako Chemicals (Richmond, VA).

Oxygen Consumption. Oxygen consumption was measured at 37 °C with stirring in the dark, using a Clark Model YSI 4004 electrode (Yellow Springs Instruments). For all assays of arachidonate or linoleate oxidation, 7.3 mM fatty acid was routinely added to 2 mL phosphate buffer (50 mM, pH 7.4) containing 0.2% sodium cholate and 100 μM diethylenetriaminepentaacetic acid (DTPA). Oxidation was initiated by addition of 11 mM ABAP. Liposomes (3.9 mM), prepared from 1-stearoyl-2-linoleoylphosphatidylcholine (*5*) were oxidized in 2 mL of phosphate buffer using 11 mM ABAP. Methyl linoleate (114 mM) was oxidized in methanol using 33.6 mM AMVN. Cholesteryl linoleate (77 mM) was oxidized in 2-propanol using 22 mM AMVN. At various time points during oxygen uptake, additions of $^{\bullet}NO$ (from an anaerobic solution using a gastight Hamilton syringe) or α-tocopherol (in absolute ethanol, final concentration in experiments = 0.25%) were made.

Measurement of Nitric Oxide. Anaerobic solutions of $^{\bullet}NO$ were prepared by equilibrating $^{\bullet}NO$ gas (Matheson, Madison, WI) in argon-saturated deionized water. Any $^{\bullet}NO_2$ present was eliminated by first bubbling $^{\bullet}NO$ through 5 M NaOH. Nitric oxide was measured by electrochemical detection using a $^{\bullet}NO$ sensor (Iso-NO, WPI Inc., Sarasota, FL). Electrode response calibration was done by measuring $^{\bullet}NO$ liberated from $KNO_2/KI/H_2SO_4$, using the following reaction performed under anaerobic conditions: $2KNO_2 + 2KI + 2H_2SO_4 \rightarrow 2NO + I_2 + 2H_2O + 2K_2SO_4$ (*15*).

Kinetic Simulations. Kinetic simulations, using the Euler method, were performed with software written by Frank Neese, Facultät für Biologie, Universität Konstanz, Germany. This algorithm uses numerical methods to solve the simultaneous differential equations generated from the proposed reaction mechanisms (Table 1).

RESULTS

Kinetics of Azo-Initiated Lipid Peroxidation. In the absence of linoleate, oxygen uptake from 11 mM ABAP decomposition (reactions 1 and 2, Table 1) was 0.78 μM/min (not shown). This gives a first order rate constant for ABAP decomposition of 1.2×10^{-6} s^{-1}, close to the published value (Table 1). In the presence of 7.3 mM linoleate the rate of oxygen uptake increased due to the propagation reactions of lipid peroxidation (Figure 1A; reactions 3−5, Table 1). Termination of peroxidation via radical−radical reactions results in inhibition of propagation and oxygen consumption (reactions 6−8, Table 1).

In this mechanism, oxygen uptake is described by the equations (*16*, *17*)

$$-dO_2/dt = k_p[ROO^{\bullet}][LH] \quad (1)$$

and

$$-dO_2/dt = [k_p/(2k_t)^{0.5}][LH]R_i^{0.5} \quad (2)$$

where k_p is the rate constant for propagation, k_t is the rate constant for termination, and R_i is the rate of initiation determined by the inhibitor method (*16*) as follows:

$$R_i = n[ArOH]/T_{inh} \quad (3)$$

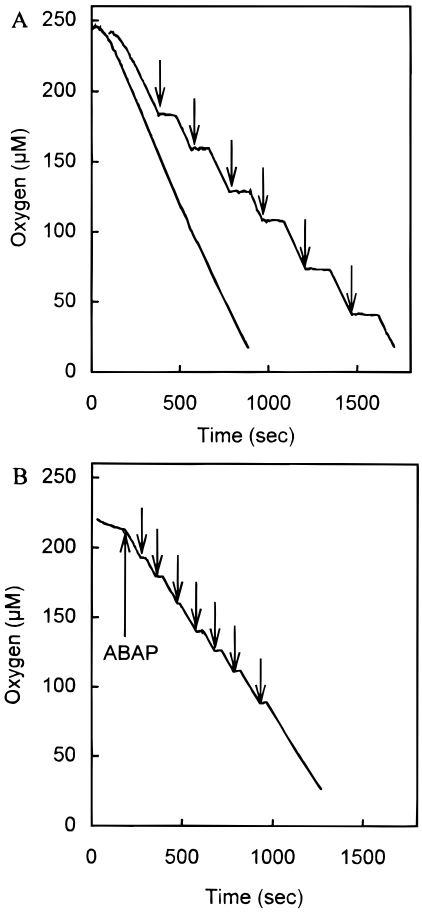

FIGURE 1: Nitric oxide inhibits oxygen uptake during ABAP-mediated oxidation of linoleate. (A) Oxidation of 7.3 mM linoleate in phosphate buffer containing 0.2% cholate and 100 μM DTPA by 11 mM ABAP was monitored using a Clark type oxygen electrode at 37 °C. Additions of 4.9 μM •NO were made as indicated at arrows (right trace). A control trace is shown on the left. (B) Oxidation of 15.9 mM 1-stearoyl-2-linoleoylphosphatidylcholine liposomes in phosphate buffer containing 100 μM DTPA by 11 mM ABAP was monitored using a Clark type oxygen electrode at 37 °C. Additions of 0.91 μM •NO were made as indicated at arrows.

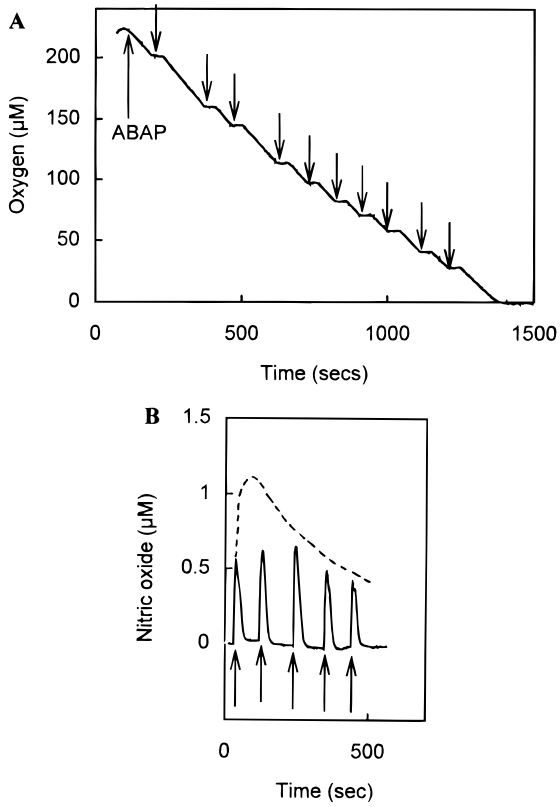

FIGURE 2: Nitric oxide consumption parallels inhibition of oxygen uptake during ABAP oxidation of linoleate. Oxygen uptake and •NO concentration was monitored during oxidation of linoleate by ABAP in room air-equilibrated buffer, as described in Figure 1. Additions of 0.91 μM •NO were made at points indicated by arrows. (A) Oxygen uptake was monitored using a Clark type oxygen electrode. (B) Nitric oxide concentration was monitored using an •NO sensor (Iso-NO, WPI Inc.). Dashed line shows disappearance of 0.91 μM •NO in the absence of linoleate or ABAP.

Here, T_{inh} is the induction period and n, the stoichiometric factor, is the number of peroxyl radicals trapped per antioxidant molecule. To calculate R_i, a known concentration of chain-breaking phenolic antioxidant (ArOH) that terminates two oxidation chains (i.e. $n = 2$) was added and the length of time was measured during which oxidation is suppressed (T_{inh}). In the reactions used herein, R_i was calculated at 7.57×10^{-9} M s^{-1} using α-tocopherol (mean of four determinations, see Figure 4). This reaction also allows calculation of k_p, the rate of propagation, according to

$$k_{inh} = k_p[LH]/R_{inh}T_{inh} \quad (4)$$

where R_{inh} is the rate of oxidation in the presence of antioxidant (found to be 4.49 μM/min at 0.96 μM α-tocopherol) and k_{inh} is the rate constant of peroxyl radical trapping [5×10^5 M^{-1} s^{-1} for α-tocopherol, (*17*)]. Using this method, k_p was determined to be 1.27×10^3 M^{-1} s^{-1}.

Nitric Oxide Inhibits Oxygen Uptake during Lipid Peroxidation Reactions Initiated by Azo Initiators. Addition of •NO from an anaerobic solution completely inhibited oxygen uptake during ABAP-initiated linoleic acid peroxidation (Figure 1A). Similar results were obtained when linoleic acid was replaced with either 1-stearoyl-2-linoleoylphosphatidylcholine liposomes (Figure 1B), arachidonate, methyl linoleate (oxidized in methanol with AMVN), or cholesteryl linoleate (oxidized in 2-propanol with AMVN) as oxidizable fatty acid substrates (not shown). Figure 2 illustrates parallel experiments in which both oxygen (Figure 2A) and •NO (Figure 2B) were measured. It was observed that in the presence of •NO, oxidation was totally inhibited and did not restart until the concentration of •NO had dropped to almost zero.

In addition to reaction with LOO•, •NO may react with other components of the lipid oxidation system, such as AOO•, A•, L•, and oxygen. However, the following conditions ensured that the reaction of •NO with LOO• was favored:

(i) ABAP-Derived Peroxyl Radicals (AOO•). The oxidation system was devised to have a kinetic chain length of 26 [i.e. $R_i/(dO_2/dt)$]. Therefore, at steady state rates of oxygen uptake, [LOO•] is 26-fold higher than [AOO•], favoring reaction of •NO with LOO• over AOO•. In agreement with this calculation, computer simulation (shown in detail later) predicted steady state concentrations of LOO• and AOO• at 27 and 1.4 nM, respectively.

(ii) Lipid or ABAP-Derived Alkyl Radicals (L• or A•). The rate of reaction of oxygen with these species is fast (10^8−10^9 M^{-1} s^{-1}). As the O_2 and •NO concentrations are 100−

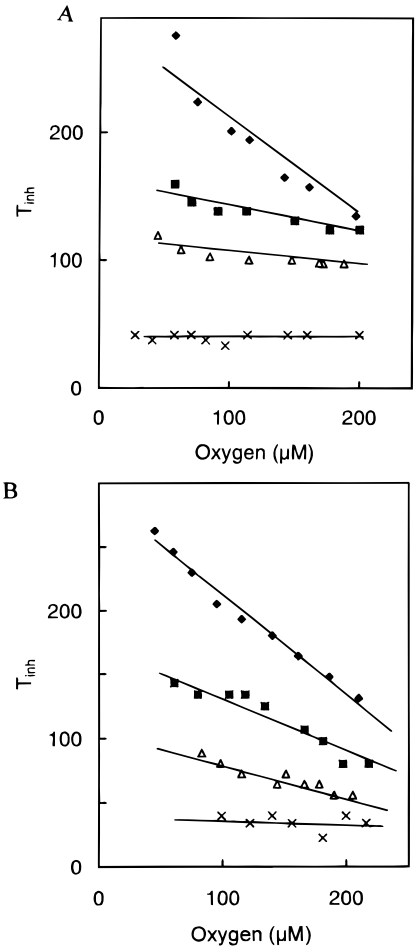

FIGURE 3: The influence of oxygen concentration on •NO inhibition of oxygen uptake. (A) Oxidation of linoleate by ABAP was monitored as described in Figure 1. (B) Oxidation of 1-stearoyl-2-linoleoylphosphatidylcholine by ABAP was monitored as described in Figure 1. Nitric oxide was added at various oxygen concentrations and time of inhibition (T_{inh}) determined. On each panel, •NO concentrations are as follows: ×, 0.91 μM; △, 2.7 μM; ■, 4.57 μM; ◆, 9.1 μM.

240 and 1−2 mM, respectively, the reaction of •NO with alkyl radicals will occur to a negligible extent.

(iii) Oxygen (O_2). The reaction between •NO and O_2 will lead to formation of additional species (NO_2/N_2O_3) capable of initiating lipid oxidation. To determine whether this reaction was taking place under our experimental conditions, we examined the time of inhibition (T_{inh}) over a range of O_2 concentrations. At •NO concentrations >1−1.5 μM, the T_{inh} was found to become progressively longer (Figure 1B). A plot of T_{inh} versus O_2 at several •NO concentrations illustrates that below 1−1.5 μM •NO, rates of peroxidation are sufficiently fast to ensure that all •NO is consumed via reaction with lipid and/or ABAP-derived peroxyl radicals (Figure 3). Therefore, for all kinetic analyses of •NO−lipid radical reactions, •NO concentrations of ≤1 μM or less were used.

Stoichiometry of the Reaction between •NO and ROO•. To address the mechanism of reaction between •NO and ROO•, three independent approaches were used: (a) calculation of the stoichiometric factor (n) by comparison of T_{inh} produced by a known concentration of lipophilic antioxidant (ArOH) with •NO, (b) measurement of •NO consumption rates in the presence of ABAP, and (c) computer simulation of the reaction between •NO and ROO•.

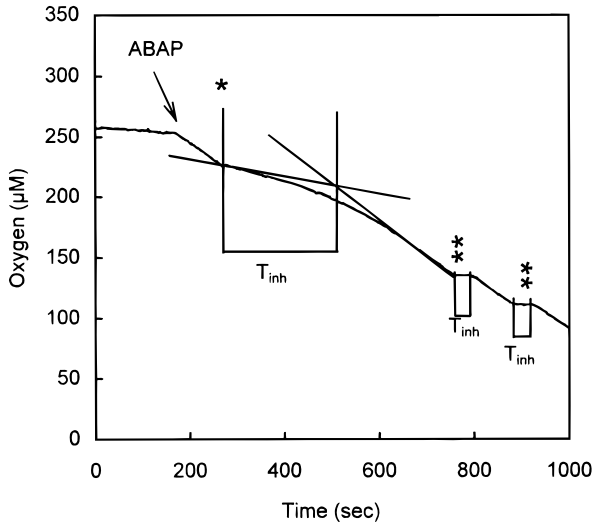

FIGURE 4: Calculation of the stoichiometric factor for •NO inhibition of oxidation, using α-tocopherol. During oxidation of 7.3 mM linoleate by 11 mM ABAP (detailed in Figure 1), the time of inhibition (T_{inh}) for 0.96 μM α-tocopherol (added at *) or 0.91 μM •NO (added at **) was determined.

(a) Calculation of the Stoichiometric Factor by Comparison of •NO and α-Tocopherol Inhibition of Propagation Reactions. In the presence of antioxidant, a new steady state approximation is applied:

$$R_i = k_{inh} n[\mathrm{ArOH}][\mathrm{ROO}^\bullet] \quad (5)$$

Substituting for [ROO•] into eq 1 gives

$$\frac{-\mathrm{d}O_2}{\mathrm{d}t} = \frac{k_p}{k_{inh}} \frac{R_i[\mathrm{LH}]}{n[\mathrm{ArOH}]} \quad (6)$$

Due to the rapid rate of reaction between •NO and peroxyl radicals [$k_{inh} = 2 \times 10^9$ M^{-1} s^{-1} (*14*)], it was anticipated, and indeed observed, that total cessation of peroxidation occurs upon addition of •NO. The fast reaction of •NO with LOO• was illustrated by comparing the effect of a similar concentration of α-tocopherol, which has a k_{inh} for reduction of LOO• to LOOH of 5×10^5 M^{-1} s^{-1} (Figure 4). Substitution of T_{inh} for •NO into eq 3 gives a stoichiometric factor for •NO of 0.310 ± 0.016 (mean ± SD, $n = 4$). This indicates that to terminate as many peroxyl radicals as α-tocopherol, 6 molar equivalents of •NO is required. However, this analysis assumes that •NO acts like α-tocopherol, which can only scavenge radicals within the lipid phase. Since it is more likely that •NO scavenges peroxyl radicals in both the lipid and aqueous phases, the stoichometic factor was recalculated using the rate of AOO• generation (1.3×10^{-8} M s^{-1}), rather than R_i, and found to be 0.515 ± 0.027. This indicates that two molecules of •NO are consumed per termination reaction.

(b) Nitric Oxide Consumption Rates. Due to the high rate constant for reaction of •NO with ROO•, •NO (0.91 μM) added to peroxidizing lipid solutions should react with ROO• ($k_{inh} = 2 \times 10^9$ M^{-1} s^{-1}) already present and decrease the steady state concentration of ROO• from 27.4 nM to near zero (13.4 pM, using eqs 1 and 5). Following this, inhibition of oxygen consumption during T_{inh} will be due to prevention of initiation via reaction of •NO with AOO•. To compare rates of •NO consumption with oxygen uptake, ABAP alone

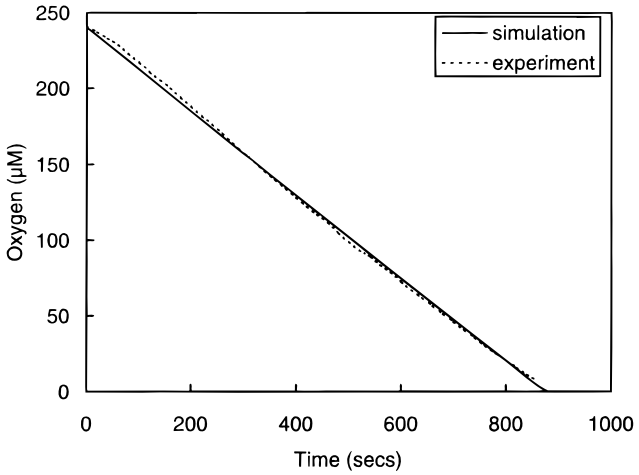

FIGURE 5: Comparison of experimental and simulated data for oxygen uptake during ABAP oxidation of linoleate. Oxygen uptake during oxidation of 7.3 mM linoleate by 11 mM ABAP was simulated using reactions and rate constants shown in Table 1 (solid line). An experimental trace obtained by oxidation of 7.3 mM linoleate by 11 mM ABAP in phosphate buffer, pH 7.4, containing 0.2% cholate and 100 μM DTPA, is shown for comparison (dashed line).

was used as a source of AOO$^\bullet$, allowing comparison with oxygen uptake when the excess of O_2 concentration ensures that $^\bullet$NO does not appreciably react with A$^\bullet$. At an oxygen uptake rate of 0.78 μM/min (ABAP, 11 mM), the rate of $^\bullet$NO consumption was 1.48 $\pm$ 0.2 μM/min (mean $\pm$ SD, n = 13), indicating that for each ABAP peroxyl radical generated, approximately two molecules of $^\bullet$NO are consumed. It should be noted that ABAP alone cannot serve as a substrate for chain propagation reactions.

(c) Computer Simulation of $^\bullet$NO-Dependent Inhibition of Peroxidation. The kinetics of oxygen uptake during oxidation of linoleic acid by ABAP was calculated by numerical integration of the differential rate equations derived from reactions 1−8 (Table 1). The rate constant for k_p (reactions 3 and 5) was calculated by substitution of experimental data into eq 4. From this, (a) oxygen uptake by ABAP alone (simulation = 0.84 μM/min, experimental = 0.78 μM/min for 11 mM ABAP), (b) oxygen uptake of ABAP plus linoleate (Figure 5), and (c) steady state concentrations of ROO$^\bullet$ (simulation = 28.4 nM, experimental = 27.4 nM) could be modeled and compared with experimental data.

For simulation of $^\bullet$NO reaction with peroxyl radicals, reactions 9−12 (Table 1) were considered. For reactions 9 and 10, the rate constant for reaction between 2-hydroxy-1-methylethylperoxyl radical and $^\bullet$NO was used (*14*), since rate constants for the reaction between lipid or ABAP peroxyl radicals and $^\bullet$NO were not available. On the basis of previous work (*24*), consumption of a second $^\bullet$NO via reaction with an alkoxyl radical, RO$^\bullet$, which would form following decomposition of ROONO to RO$^\bullet$ and $^\bullet NO_2$, is proposed. Since the rate of decomposition of ROONO is not known, the composite reaction between $^\bullet$NO and ROONO to give RONO was modeled using a range of rate constants between 0 (stable ROONO products) and 2×10^9 M^{-1} s^{-1} [rate of $^\bullet$NO + RO$^\bullet$ reaction (*18*)] and compared with experimental data.

Since the kinetic simulation program allowed addition of reactants only at $t = 0$, the reaction was first simulated in the absence of $^\bullet$NO (Table 2), allowing calculation of

Table 2: Concentrations of All Reactants Present at $t = 0$ and 200 s, during ABAP Oxidation of Linoleate, As Calculated by Reaction Simulation

reactant/intermediate	starting concn, (M) at $t = 0$ s	concn (M) at $t = 200$ s
ABAP (A−N=N−A)	1.1×10^{-2}	1.1×10^{-2}
A$^\bullet$	0	3.87×10^{-14}
O_2	2.4×10^{-4}	1.85×10^{-4}
AOO$^\bullet$	0	1.49×10^{-9}
LH	7.6×10^{-3}	7.55×10^{-3}
L$^\bullet$	0	4.87×10^{-12}
LOO$^\bullet$	0	2.67×10^{-8}

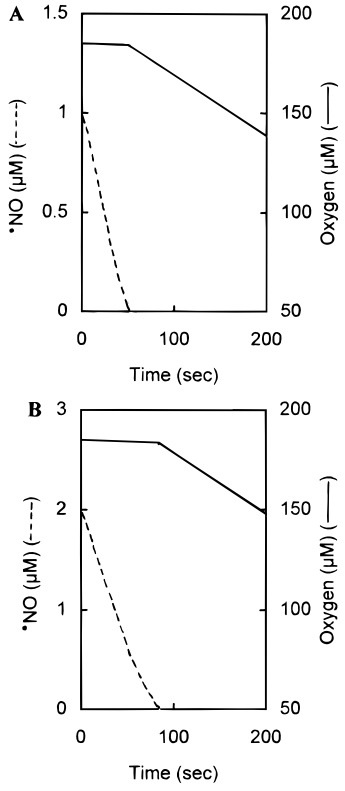

FIGURE 6: Nitric oxide consumption parallels inhibition of oxygen uptake in the kinetically simulated reaction. Nitric oxide consumption (dashed lines) and oxygen uptake rates (solid lines) were calculated using computer simulation of 11 mM ABAP oxidation of 7.3 mM linoleate as detailed under Results. For the reaction of $^\bullet$NO with ROONO, $k_{12} = 7 \times 10^4$ M^{-1} s^{-1}. At $t = 0$, various concentrations of $^\bullet$NO were added as follows: (A) 1 μM $^\bullet$NO and (B) 2 μM $^\bullet$NO.

concentrations of all reactants present during the reaction. For peroxyl radical intermediates, steady state concentrations were reached within 9 s (LOO$^\bullet$, 27 nM; AOO$^\bullet$, 1.4 nM) and did not change until the reaction became anaerobic. Alkyl radical concentrations were several orders of magnitute lower and did not increase above 0.02 nM until the system approached anoxia. Next, the simulation was repeated with various concentrations of $^\bullet$NO added at $t = 0$, but using concentrations of all other reactants determined to be present at 200 s (Table 2). As experimentally observed, $^\bullet$NO caused total cessation of oxygen uptake, which then returned to original rates when all $^\bullet$NO had been consumed (Figure 6). Plotting T_{inh} versus $^\bullet$NO concentration demonstrated a linear relationship for both experimental (slope = 43 s μM^{-1}, r = 0.998) and simulated data [e.g. with $k_{12} = 0$ (slope = 62.6 s μM^{-1}, r = 0.997) or with $k_{12} = 2 \times 10^9$ M^{-1} s^{-1} (slope = 34.6 s μM^{-1}, r = 0.999) (Figure 7)]. The closest fit to

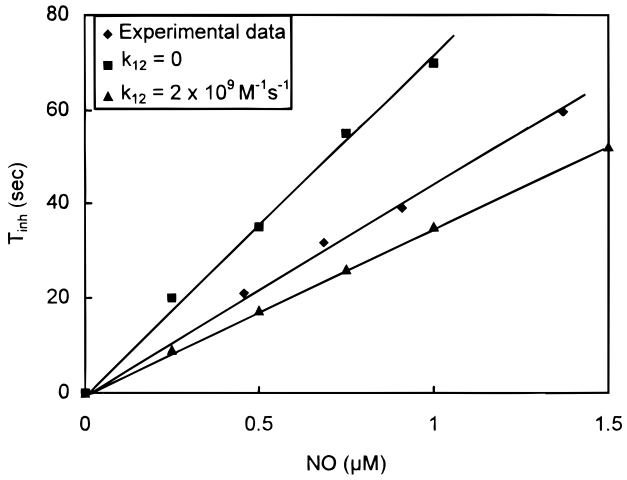

FIGURE 7: Comparison of experimental T_{inh} for •NO with those predicted from the simulated reaction. T_{inh} for •NO was determined either experimentally (described in Figure 5) or by simulation using two different values for k_{12}, in the presence of various concentrations of •NO.

the experimental data was obtained using a composite rate constant of 7×10^4 M^{-1} s^{-1} (slope = 44.7 s μM^{-1}, r = 0.977) for reaction of the second •NO.

DISCUSSION

Nitric oxide inhibits oxidative damage in numerous models ranging from biochemical to in vivo studies, including metal and cell-induced lipid peroxidation (*9*), xanthine oxidase and hyperoxic lung injury (*19*), and ischemia−reperfusion injury to various organs (*20*−*22*). The inhibition of lipid peroxidation by •NO has been proposed to contribute in part to these protective actions, via chain termination reactions with lipid peroxyl and/or alkoxyl radicals (*6*, *9*, *14*, *23*). Direct reactions between lipid radicals and •NO have not been studied in detail, with several alternative reactions for •NO existing in biological systems that might also lead to inhibition of oxidation. These include metal−nitrosyl complex formation (*12*), inhibition of lipoxygenase (*13*), and reduction of partially oxidized lipophilic antioxidants. To define reactions that explain the inhibitory effects of •NO on lipid peroxidation, this study examined the kinetics of reaction of •NO with LOO• formed during organic peroxyl radical-initiated linoleate oxidation. The reaction between LOO• and •NO led to immediate termination of oxidation and occurred at a rate consistent with previously calculated rate constants for the reaction between peroxyl radicals and •NO. Also, at least two molecules of •NO are consumed per molecule of LOO• destroyed. This antioxidant activity differs from α-tocopherol in that each α-tocopherol molecule terminates 2 lipid peroxidation chain reactions.

Reactions between a variety of peroxyl radicals [e.g. CH_3OO•, C_2H_5OO•, $(CH_3)CHOO$•, and several others] and •NO have been summarized (*23*). Rate constants (pressure independent, 10−55 °C) are all extremely high with rates ranging from 2×10^9 to 11×10^9 M^{-1} s^{-1} (*14*, *23*, *24*) being reported. These reactions were proposed to proceed predominantly, if not solely, as follows:

$$ROO^{\bullet} + {}^{\bullet}NO \rightarrow ROONO \rightarrow [RO^{\bullet}\ {}^{\bullet}NO_2] \rightarrow RO^{\bullet} + {}^{\bullet}NO_2$$

where ROONO represents an unstable intermediate that rapidly decomposes [k = 0.1−0.3 s^{-1} (*14*)] to generate a free alkoxyl radical and nitrogen dioxide (•NO_2) via a caged radical pair [RO• •NO_2] (*25*). For the reaction between •NO and C_2H_5OO•, consumption of •NO at twice the rate of •NO_2 formation has been observed (*26*), suggesting a stoichiometry of 2:1 for the •NO:C_2H_5OO• reaction. Reaction between RO• and •NO to form RONO [rate constant 3×10^9 M^{-1} s^{-1} (*18*)], an alkyl nitrite, has been suggested to account for removal of the second •NO. However, additional reactions are possible, including recombination of the caged radical pair to form $RONO_2$ [$k = 1.68 \times 10^9$ M^{-1} s^{-1} for C_2H_5OO• (*24*)], reaction of ROO• with •NO_2 to form $ROONO_2$ [$k = 3-6 \times 10^9$ M^{-1} s^{-1} (*22*)], and reaction between RO• and •NO to generate an aldehyde and HNO [e.g. $C_2H_5O^{\bullet} + {}^{\bullet}NO \rightarrow CH_3CHO + HNO$ (*24*)].

Comparison of •NO consumption and O_2 uptake by ABAP in the absence of linoleate revealed a reaction stoichiometry of 2:1 (•NO:AOO•). In the case of ABAP, reaction of AO•, formed on dissociation of AOONO, with a second •NO could give AONO as previously suggested for C_2H_5O• reaction with •NO (*26*), or •NO could react with •NO_2 to form N_2O_3. However, the overall stoichiometry indicates that non-•NO-consuming reactions for both •NO_2 and AO• are also taking place, for example, recombination to give $AONO_2$. On the basis of the stoichiometry observed, we propose the following set of reactions as consistent with the experimental observations:

$$2{}^{\bullet}NO + 2ROO^{\bullet} \rightarrow 2ROONO$$

$$2ROONO \rightarrow 2RO^{\bullet} + 2{}^{\bullet}NO_2$$

$$RO^{\bullet} + {}^{\bullet}NO_2 \rightarrow RONO_2$$

$$RO^{\bullet} + {}^{\bullet}NO \rightarrow RONO$$

$${}^{\bullet}NO + {}^{\bullet}NO_2 \rightarrow N_2O_3$$

$$N_2O_3 + H_2O \rightarrow 2HNO_2$$

$$4{}^{\bullet}NO + 2ROO^{\bullet} + H_2O \rightarrow 2HNO_2 + RONO_2 + RONO$$

In the above scheme, the reaction of •NO with RO• may occur before dissociation; that is, •NO may react with the caged radical pair [RO• •NO_2] to form RONO and free •NO_2. Similarly, the reaction of the caged radicals [RO• •NO_2] to form $RONO_2$ is likely to take place before dissociation. These alternatives will not alter the overall stoichiometry of 2 •NO consumed per ROO• generated, however. The reaction between ROO• and •NO_2 was omitted from the above scheme, since it is likely to be limited by the low concentrations of both free •NO_2 and ROO• (with ROO• concentration at 13.4 pM in the presence of •NO using eqs 1 and 5).

Comparison of T_{inh} for both α-tocopherol and •NO indicated that to terminate as many LOO• as 1 molar equivalent of α-tocopherol (which can scavenge two peroxyl radicals per mole), 6 molar equivalents of •NO is required. This difference may reflect differences in both secondary reactions of •NO and in •NO or α-tocopherol partitioning. In these experiments, it is expected that α-tocopherol and •NO will partition in the hydrophobic lipid-detergent compartment [•NO has an *n*-octanol:water partition coefficient

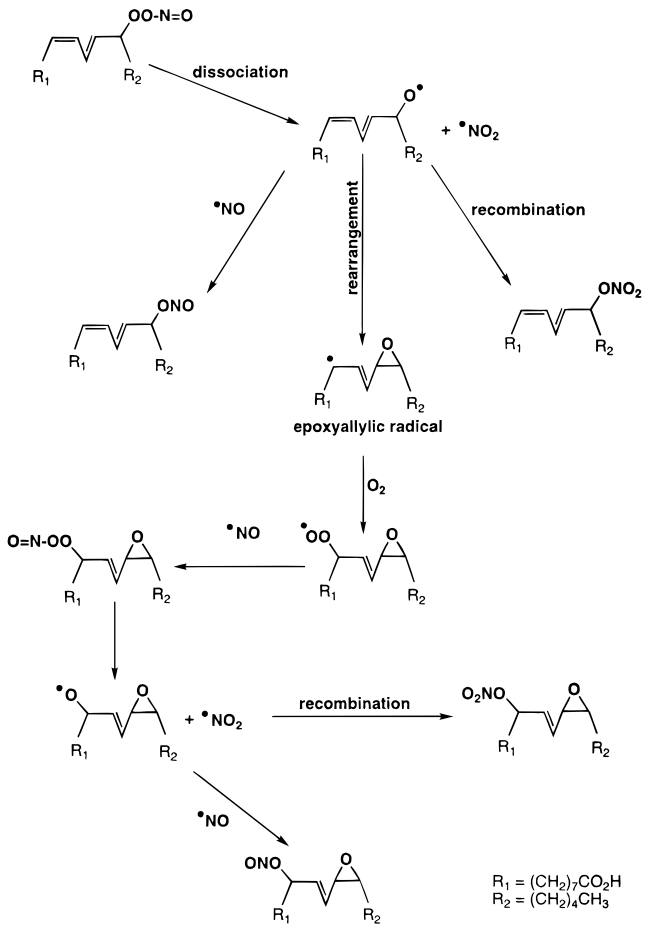

FIGURE 8: Proposed pathways for LOONO decomposition.

of 6.5:1 (*27*)]. It is likely that the reaction stoichiometry between •NO and linoleate peroxyl radicals is different from those described for other ROO•:•NO reactions. Linoleate alkoxyl radical (LO•), which will form following decomposition of the primary LOONO product, can rapidly rearrange to give an epoxyallylic carbon-centered radical [L(O)•], which reacts with oxygen to form another peroxyl radical [L(O)-OO•] (*28*). Thus, if LO• radicals rearrange to epoxyallylic radical species before reaction with •NO, consumption of additional molecules of •NO could occur via reaction with L(O)OO•, before complete termination (Figure 8). Removal of more than one •NO per LOO• indicates that additional reactions are taking place during inhibition of oxidation and that the initial products, LOONO, are not stable organic peroxynitrites. However, since •NO addition to oxidizing lipid ultimately results in complete inhibition of oxygen uptake, species that do not propagate lipid peroxidation reactions must ultimately form. Using HPLC−mass spectroscopy, stable nitrated lipid species were not detected in these experiments. This is most likely due to the low steady state concentrations of LOO• (27 nM) that are present before addition of •NO. Thus, the products of •NO−lipid radical termination reactions are below the limit of detection in these experiments. In a previous study, compounds with molecular weight consistent with LOONO were found on addition of •NO to peroxidizing lipid mixtures (*8*, *29*). These were originally interpreted as organic peroxynitrites formed as the initial termination product of LOO• with •NO. In light of this study, it is more probable that these formed following secondary reactions, for example, recombination of LO• with $•NO_2$, as shown in Figure 8.

Computer simulation of ABAP oxidation of linoleate was in close agreement with experimental data. Using a 2:1 reaction ratio (•NO:ROO•), the model predicted that a composite rate constant of 7×10^4 M^{-1} s^{-1} best approximated the reaction sequence consisting of decomposition of ROONO to RO• and reaction of this with a second •NO to form RONO. The rate constant for decomposition of the ROONO formed following reaction of •NO with the 2-hydroxy-1-methylethylperoxyl radical ($0.1-0.3$ s^{-1}) predicts a half-life of 2−6 s for this species (*14*). If the lipid product, LOONO, has a similar half-life, it is likely that decomposition to LO• is the rate-limiting step preceding reaction of the second •NO, since direct reactions between alkoxyl radicals and •NO are significantly faster at 2×10^9 M^{-1} s^{-1} (*18*).

The actions of •NO as an antioxidant in vivo will depend on both the rate and stoichiometry of reaction with peroxyl radicals, relative to that of other antioxidants, and the ability of •NO to partition within the lipid/aqueous compartments. The rate constant for α-tocopherol reaction with LOO• is 5×10^5 M^{-1} s^{-1}, with plasma concentrations of α-tocopherol being ≈20 μM. Since a 6-fold molar excess of •NO over α-tocopherol is required to give equivalent T_{inh}, steady state concentrations of 30 nM •NO would be expected to inhibit lipid oxidation to the same extent as 20 μM α-tocopherol. Following inflammatory activation of vascular cells, high local concentrations (1−2 μM) of •NO can be achieved (*30*). Therefore, during tissue oxidative stress and inflammation, •NO can predominate over α-tocopherol as a lipid peroxyl radical scavenger. In support of this concept, •NO prevents α-tocopherol depletion during oxidation of LDL (*31*).

Effective antioxidant activity of •NO against lipid peroxidation in vivo is influenced by a variety of factors. First, rates of •NO synthesis by vascular cells are variable. Unlike other lipophilic antioxidants, •NO production and delivery are highly controllable processes determined by regulation of •NO synthase (NOS) gene expression, substrate and cofactor availability, and receptor-dependent stimulation of some NOS isoforms. In contrast, tissue α-tocopherol levels and consumption during oxidative stress depend exclusively on extents of dietary intake of both α-tocopherol and ascorbate. Second, simultaneous production of $O_2•^-$ will reduce the antioxidant potency of •NO since (a) $ONOO^-$, a potent lipid oxidant, is formed as a product (*5*) and (b) less •NO will be available for reaction with lipid radicals.

In summary, we have observed the direct reaction between •NO and LOO results in potent inhibition of lipid peroxidation propagation reactions. Kinetic analysis of this reaction indicates that an antioxidant role for •NO in vivo is highly likely.

ACKNOWLEDGMENT

We thank Dr. J. P. Eiserich for helpful mechanistic discussions.

REFERENCES

1. McCartney-Francis, N., Allen, J. B., Mizel, D. E., Albina, J. E., Xie, Q. W., Nathan, C. F., and Wahl, S. M. (1993) *J. Exp. Med. 178*, 749−754.
2. Grisham, M. B., Specian, R. D., and Zimmerman, T. E. (1994) *J. Pharmacol. Exp. Ther. 271*, 1114−1121.
3. Mulligan, M. S., Moncada, S., and Ward, P. A. (1992) *Br. J. Pharmacol. 107*, 1159−1162.

4. Matheis, G., Sherman, M. P., Buckberg, G. D., Haybron, D. M., Young, H. H., and Ignarro, L. J. (1992) *Am. J. Physiol. 262*, H616−H620.
5. Radi, R., Beckman, J. S., Bush, K., and Freeman, B. A. (1991) *Arch. Biochem. Biophys. 288*, 481−487.
6. Hayashi, K., Noguchi, N., and Niki, E. (1995) *FEBS Lett. 370*, 37−40.
7. Yates, M. T., Lambert, L. E., Whitten, J. P., McDonald, I., Mano, M., Masayuki, M., Ku, G., and Mao, S. J. T. (1992) *FEBS Lett. 309*, 135−138.
8. Rubbo, H., Radi, R., Trujillo, M., Telleri, R., Kalyanaraman, B., Barnes, S., Kirk, M., and Freeman, B. A. (1994) *J. Biol. Chem. 269*, 26066−26075.
9. Hogg, N., Kalyanaraman, B., Joseph, J., Struck, A., and Parthasarathy, S. (1993) *FEBS Lett. 334*, 170−174.
10. Wink, D. A., Cook, J. A., DeGraff, W., Gamson, J., Liebman, J., Krishna, M. C., and Mitchell, J. B. (1996) *Arch. Biochem. Biophys. 331*, 241−248.
11. Pfeiffer, S., Gorren, A. C. F., Schmidt, K., Werner, E. R., Hansert, B., Bohle, D. S., and Mayer, B. (1997) *J. Biol. Chem. 272*, 3465−3470.
12. Traylor, T. G., and Sharma, V. S. (1992) *Biochemistry 31*, 2847−2849.
13. Kanner, J., Harel, S., and Granit, R. (1992) *Lipids 27*, 46−49.
14. Padmaja, S., and Huie, R. E. (1993) *Biochem. Biophys. Res. Commun. 195*, 539−544.
15. Instruction Manual (1996) ISO-NO and ISO-NO Mark II, Isolated nitric oxide meters and sensors, World Precision Instruments, Inc., Sarasota, FL.
16. Boozer, C. E., Hammond, G. S., Hamilton, C. E., and Sen, J. N. (1955) *J. Am. Chem. Soc. 77*, 3233−3237.
17. Niki, E., Saito, T., Kawakami, A., and Kamiya, Y. (1984) *J. Biol. Chem. 259*, 4177−4182.
18. Frost, M. J., and Smith, I. W. M. (1990) *J. Chem. Soc., Faraday Trans. 86*, 1757−1762.
19. Guttierez, H. H., Nieves, B., Chumley, P., Rivera, A., and Freeman, B. A. (1996) *Free Radical Biol. Med. 21*, 43−52.
20. Dawson, V. L., Dawson, T. M., London, E. D., Bredt, D. S., and Snyder, S. H. (1991) *Proc. Natl. Acad. Sci. U.S.A. 88*, 6368−6371.
21. Jessup, W., Mohr, D., Gieseg, S. P., Dean, R. T., and Stocker, R. (1992) *Biochim. Biophys. Acta 1180*, 73−82.
22. Malo-Ranta, U., Yla-Herttuala, S., Metsa-Ketela, T., Jaakkok, O., Moilanen, E., Vourinen, P., and Nikkari, T. (1994) *FEBS Lett.* 179−183.
23. Wallington, T. J., Dagaut, P., and Kurylo, M. J. (1992) *Chem. Rev. 92*, 667−710.
24. Maricq, M. M., and Wallington, T. J. (1992) *J. Phys. Chem. 96*, 986−992.
25. Pryor, W. A., Castle, L., and Church, D. F. (1985) *J. Am. Chem. Soc. 107*, 211−217.
26. Maricq, M. M., and Szente, J. J. (1996) *J. Phys. Chem. 100*, 12374−12379.
27. Malinski, T., Taha, Z., Grunfeld, S., Patton, S., Kapturczak, M., and Tomboulian, P. (1993) *Biochem. Biophys. Res. Commun. 193*, 1076−1082.
28. Wilcox, A. L., and Marnett, L. J. (1993) *Chem. Res. Toxicol. 6*, 413−416.
29. Rubbo, H., Parthasarathy, S., Barnes, S., Kirk, M., Kalyanaraman, B., and Freeman, B. A. (1995) *Arch. Biochem. Biophys. 324*, 15−25.
30. Malinski, T., Bailey, F., Zhang, Z. G., and Chopp, M. (1993) *J. Cereb. Blood Flow Metab. 13*, 355−358.
31. Goss, S. P. A., Hogg, N., and Kalyanaraman, B. (1995) *Chem. Res. Toxicol.* 8, 800−806.
32. Wink, D. A., Darbyshire, J. F., Nims, R. W., Saavedra, J. E., and Ford, P. C. (1993) *Chem. Res. Toxicol. 6*, 23−27.
33. Niki, E., Saito, M., Yoshikawa, Y., Yamamoto, Y., and Kamiya, Y. (1986) *Bull. Chem. Soc. Jpn. 59*, 471−477.
34. Babbs, C. F., and Steiner, M. G. (1990) *Free Radical Biol. Med. 8*, 471−485.

BI971891Z